# Analysis of the Effect of Partial Transmission Element on the Performance of Fano Laser


Mohammad Heydari
MSc Student
Faculty of engineering
Shahed University
Tehran, Iran, Zipcode: 3319118651
mohammad.heydari@shahed.ac.ir

MohammadHasan Yavari
Assistant Professor
Faculty of engineering
Shahed University
Tehran, Iran, Zipcode: 3319118651
mh.yavari@shahed.ac.ir

Aref Rasoulzadeh Zali
PhD Student
IPI-ECO Research Institute
Eindhoven University of Technology
Eindhoven, the Netherlands
a.rasoulzadehzali@tue.nl



***Abstract*—In this paper, we investigate the effect of the partial transmission element on the output power dynamics of the Fano laser. By changing the radius of the holes in the photonic crystal waveguide, the reflection coefficient and symmetry of the Fano mirror change. Moreover, by adjusting partial transmission element radius, we show that it is possible to enhance the output power, without increasing the laser pumping current. It has been shown that by increasing the radius of the partial transmission element, the reflection rate in the Fano mirror is increased which enhances the laser output power from 25 mW to 400 mW.**



**Keywords— partial transmission element, Fano laser**


## I. INTRODUCTION

Nowadays with the rapid development of the ultrahigh-bit-rate optical systems, the production of ultra-short optical pulses [1], with a very high repetition rate, is essential [2]. Nanocavity lasers based on Photonic Crystals (PhC) can be used in photonic integrated circuits thanks to their small size, low power consumption, and different mode of operations including, continuous and pulse regimes[2,6]. PhC nanocavities with very high-quality factor in a very small cavity volume enhance the Purcell coefficient, which increases the spontaneous emission coupling to the lasing mode. It makes decreasing the threshold current and makes the realization of ultra-compressed lasers feasible [6-9]. Small mode volume in the photonic crystal nanocavities [8] and high group-velocity dispersion in PhC waveguides [9] lead to slow light phenomena [10] and increasing of the light-material interaction (LMI) [11]. Consequently, the power consumption of PhC is highly decreased. One type of photonic crystal lasers based on Fano resonance was recently introduced in 2014 [12]. Fano resonance [13] is interference between a continuum of waveguide mode and a discrete mode level [14], which occurs in many quantum and classical systems[17,18].

## II. STRUCTURE

### A. Fano Laser Structure

According to Refs. [18–20], the photonic crystal Fano laser (FL) is created based on a photonic crystal semiconductor InP membrane with periodically placed triangular air-holes, c.f. in Fig. 1. In the Fano laser, nanocavity can be created by removing a hole (H1-type) or moving holes (H0-type). Here, H1-type nanocavity, which is created by removing a hole. The left mirror is created by the blockade of the waveguide by air-holes, and the right mirror is created by the interference between the continuum of waveguide modes and the discrete mode of the nanocavity.

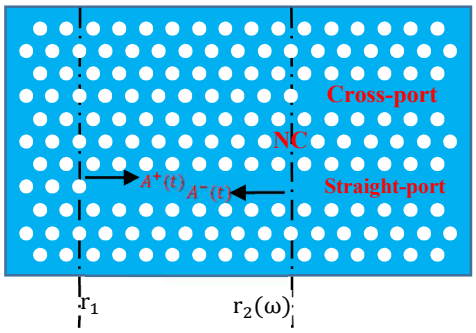


Fig. 1. The Fano laser structure, wherein $r_1$ and $r_2(\omega)$ represent the corresponding reflectances at the left and right mirrors.

The active region of the laser is composed of InAs quantum dots and is confined to a direct waveguide between the left and right mirrors. $A^+$ and $A^-$ are the envelopes of the right and left propagating fields, and NC represents the nanocavity. The laser also has two cross-port and straight-port outputs, the cross-port is intended only to increase the output power [4], [8], [18-20].

### B. PTE Structure

The partially transmitting element (PTE), as shown in Fig. 2, is located below the nanocavity, thereby controlling the amplitude and phase of the Fano mirror reflection coefficient perturbing the interference between the waveguide propagating field and nanocavity field, which controls the phase and amplitude of the transmission spectrum.

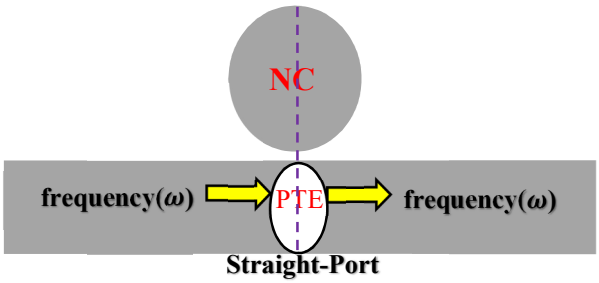


Fig. 2. the location of the PTE. The PTE is exactly in symmetry considering, the mid-plane.

By changing the radius of air-hole PTE embedded below the nanocavity one could achieve a variable reflection coefficient $r_B$ which, in addition to controlling the amplitude


978-1-6654-3365-5/21/$31.00 ©2021 IEEE

of the transmission spectrum, could control the symmetry of the generated Fano shape. Indeed, $r_B = 0$ indicates asymmetric Fano resonance and, $r_B \neq 0$ indicates asymmetric Fano resonance. The relationship between the reflection amplitude coefficient ($r_B$) and the transmission amplitude coefficient ($t_B$) can be expressed as the following equation:

$$t_B = \sqrt{1 - r_B^2} \tag{1}$$

In the absence of a blocking hole (PTE) in the structure, there is an expectation of full transmission of the spectrum to the output, which due to a back-scattered field, there will be a dip in the transmission and a corresponding reflection peak[19].

## III. Simulation Results And Discussion

In the steady-state, the laser oscillation condition can be expressed as follows [20]:

$$r_1 r_2(\omega) \exp[2ikL] = 1 \tag{2}$$

To solve the above equation, it is assumed that there is no carrier density in the nanocavity (the nanocavity is passive), meaning that there is no excitation of carriers in the nanocavity. $r_1$, $r_2(\omega)$ are the reflection coefficients of the left and right mirrors, respectively. $L$ is the effective length, and $k$ is the complex wavenumber. Solving the oscillation condition will lead to the creation of amplitude and phase conditions of electric fields, as follows[18,19]:

$$g(\omega_s, N_s) = \alpha_i + \frac{1}{2L} \ln\left(\frac{1}{R_1(\omega) + R_2(\omega_s, \omega_c)}\right) \tag{3}$$

$$\arg\{r_1(\omega_s)\} + \arg\{r_2(\omega_s, \omega_c)\} + \frac{2\omega_s}{c} n(\omega_s, N_s) L = 2\pi p \tag{4}$$

The steady-state value of the reflection coefficient (for a given $\omega_c$ that is a free parameter) is the value where $\delta = \omega_s - \omega_c$, and $\omega_s$ is the solution to the oscillation condition found for that choice of $\omega_c$. That means the steady-state value of $r_2(\omega)$ changes when choosing a new resonance frequency of the nanocavity. The equation $r_2(\omega)$ can be expressed as the following equation.

$$r_2(\omega_s, \omega_c) = r_B + (\mp i t_B - r_B) \left(\frac{-p\gamma_c}{i\delta_c + \gamma_T - \frac{1}{2}(1 - i\alpha)\Gamma_c v_g g_N (N_c - N_0)}\right) \tag{5}$$

$p$ is the parity of the cavity mode, $\gamma_c$ is coupling to the waveguide, $\delta_c$ is the detuning, $\gamma_T$ is the total decay rate, $\alpha$ is the linewidth enhancement factor, $\Gamma c$ is the nanocavity confinement factor, $v_g$ is the group velocity, $g_N$ is the differential gain, $Nc$ is the nanocavity carrier density, and $N_0$ is the transparency carrier density of the active material. Also, in Fano laser, the equations of forward field, backward field, waveguide carrier density, and nanocavity carrier density are as follows[18,20]:

$$\frac{dA^+(t)}{dt} = \frac{1}{2}(1 - i\alpha)\Gamma v_g g_N (N(t) - N_s) A^+(t) + \gamma_L \left[A^-(t)/r_2(\omega_c, \omega_s) - A^+(t)\right] \tag{6}$$

$$\frac{dA^-(t)}{dt} = (-i\Delta\omega - \gamma_T) A^-(t) - p\gamma_c A^+(t) + \frac{1}{2}(1 - i\alpha)\Gamma_c v_g g_N (N_c(t) - N_s) A^-(t) \tag{7}$$

$$\frac{dN(t)}{dt} = \frac{J}{eV_C} - R(N) - \Gamma_C v_g g_N (N(t) - N_S)\sigma_S \frac{A^+(t)}{V_{LC}} \tag{8}$$

$$\frac{dN_C(t)}{dt} = -\frac{N_C(t)}{\tau_c} - \Gamma_c v_g g_N (N_C(t) - N_0) \frac{\rho |A^-(t)|^2}{V_{NC}} \tag{9}$$

where $\gamma_L$ is inverse of the cavity roundtrip time, $J$ is current, $V_{LC}$ is the volume of the laser cavity, $R(N)$ is the recombination rate, $\sigma_s$ is a parameter relating to photon number . Solving the above equations using the Runge-Kutta method results in laser operation in both pulsed and continuous regimes.

### A. The Effect of the PTE on the Fano Mirror Properties

In this section, we will simulate PTE's effect on the reflection spectrum of a Fano mirror. Based on Fig. 3, it can be seen that the reflection spectrum in the state $r_B = 0$ is a Lorentzian spectrum which is symmetric spectrum. The corresponding transmission spectrum will have a dispersion caused by the back-scattered field. Indeed, a narrowband, single-mode, and dispersive mirror create based on the interference between the waveguide and the cavity in this situation. As the radius of the blocking air-hole increases, the spectrum changes from symmetric to asymmetric shape, and this asymmetry in the Fano laser is determined solely by $r_B$. By increasing $r_B$ from 0.2 to 0.8, a Fano spectrum is created based on what has been described before. Fano shape spectrum has an on-off transition, so this transition contrast will be sharpened by increasing the radius of the air-hole, and since in applications such as switches, the higher contrast of the spectrum means faster switching process in switches. At $r_B = 1$ the spectrum has a symmetric inverse Lorentzian shape, and the dip in the reflection spectrum corresponds to a peak in the transmission spectrum. In the case where $r_B = 1$, the spectrum is not transmitted directly from the straight-port to the output, and the only way to transfer the spectrum to the output is through nanocavity, and that occurs at the resonance. According to Fig. 3(b), which shows the phase of the Fano spectrum, in the spectrum phase, we will only see a slight frequency shift for different $r_B$ [20-22].

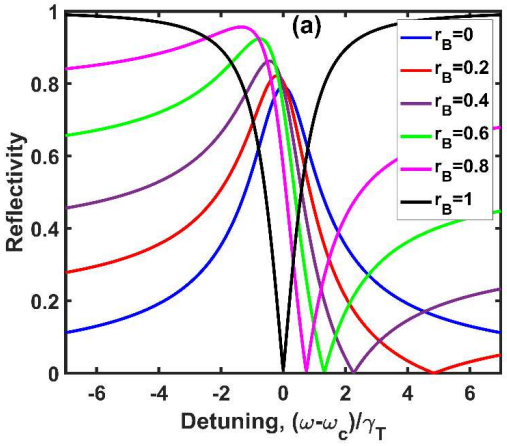

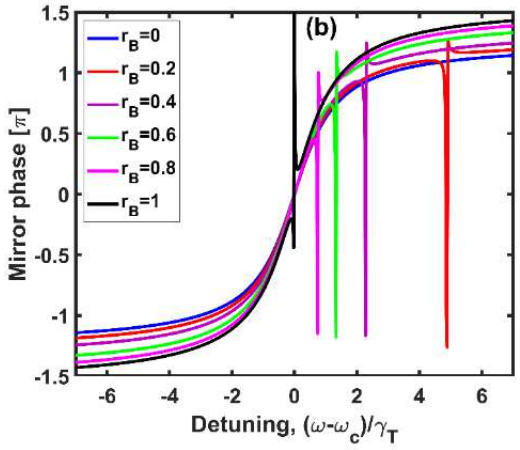


Fig. 3. The reflection spectrum of the Fano mirror is based on the radius of the different air-holes $r_B$. (a) The amplitude spectrum (b) The phase spectrum

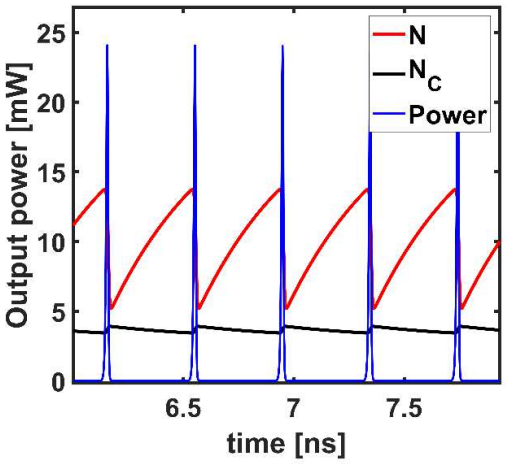


Fig. 4. Waveguide and nanocavity carrier density as well as the output power of self-pulsed Fano laser [18].

### B. *The Effect of the PTE on the Fano Laser Output*

Since the purpose of this paper is to increase the laser output power in the pulse regime, it is necessary to investigate the laser output, thus we will model equations 6 to 9 based on the parameters in Table 1.

Table 1. Parameters used for numerical simulation[18].

| Parameter | Symbol | Value | Unit |
|---|---|---|---|
| wavelength | $\lambda_r$ | 1554 | nm |
| Cavity length | $L$ | 5 | µm |
| Nanocavity volume | $V_{NC}$ | 0.24 | $\mu m^3$ |
| Transparency carrier density | $N_0$ | $1\times10^{24}$ | $m^{-3}$ |
| Differential gain | $g_N$ | $5\times10^{-20}$ | $m^2$ |
| Internal loss | $\alpha_i$ | 1000 | $m^{-1}$ |
| Nanocavity carrier lifetime | $\tau_c$ | 0.5 | ns |
| Phase and group indices | $n,n_g$ | 3.5 | |
| confinement factor | $\Gamma$ | 0.5 | |
| Linewidth enhancement factor | $\alpha$ | 1 | |
| Total Q-factor | $Q_T$ | 500 | |
| Intrinsic Q-factor | $Q_i$ | 14300 | |
| Cross-port Q-factor | $Q_p$ | 10000 | |
| Left mirror reflectivity | $R_1$ | 1 | |

As shown in Fig. 4, periodic changes in output power follow changes in carrier densities in waveguides and nanocavity. In laser self-pulsation regime operation, the active waveguide is optically pumped at a constant intensity, while the nanocavity is passive, which acts as a saturable absorber. By increasing the carrier density, the optical field intensity increases inside the waveguide. When the field intensity increases, the absorption of the saturable absorber decreases and allows the pulse peak to evolve. On the other hand, by reducing the carrier density to lower than the threshold, the lasing will stop, and the tailing of the pulse will develop as well. Again, the injected current into the active region of the laser increases the waveguide carrier density, and the next pulse will appear as shown in Fig. 4, and the process will continue in the same way. This process will take place due to the saturation of quantum dots in the nanocavity and eventually decreasing the absorption in the nanocavity; as a result, the intensity of the mirror reflectivity increases because of the reduction in mirror loss which increases the intensity of the optical field inside the laser main cavity. Consequently, based on what has been shown in Fig. 4, one could see a pulse evolution in the laser output. Periodic changes in the reflection coefficient of the Fano mirror will produce a pulse at the laser output. Fig. 5 shows the reflection coefficient of a Fano mirror in two modes with oscillation and non-oscillation behavior. Periodic changes in the reflection coefficient of the Fano mirror indicates the saturation of the nanocavity. The blue curve shows that the reflection is constant and in this case pulse will not be produced at the output.[18-20].

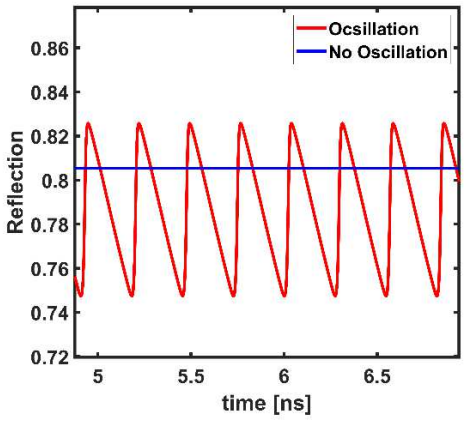


Fig. 5. Fano reflection coefficient in oscillation and non-oscillation conditions[17].

Increasing the pumping current of the laser active region, and confinement of the nanocavity will increase the waveguide carrier density and the nanocavity. This will result in the excitation of more photons in the nanocavity, which increases the nonlinear effects and increase the laser output power. Another factor affecting the increase of laser output power is increasing the linewidth enhancement factor which will increase the detuning which could increase the laser output

power in the pulse regime. All the above-mentioned factors restrict the laser performance. For instance, with a small increase in them, the laser output power will change from a pulsation to a continuous wave regime, which in many applications is not desirable[22-23].

Applying a PTE is an important way to maintain the pulse state of the laser and increase the output power much more compared to the previously mentioned parameters. The placement of the PTE will be possible only by making the geometric change in the structure of the laser. Fig. 6 illustrates the effects of applying a partial transition element on the Fano laser output power. As depicted, it is observed that the laser output power in the case of $r_B = 0$ is equal to 25 mW. By increasing to larger values (at 0.4 and 0.8), the laser output power has a relatively large increase. However, by increasing $r_B$ to 1, the laser maximum output power will reach nearly 400 mW. In this case, the current has a constant value of 1.2 mA. As a result, by applying the partial transmission element one could further optimize and increase the laser output power.

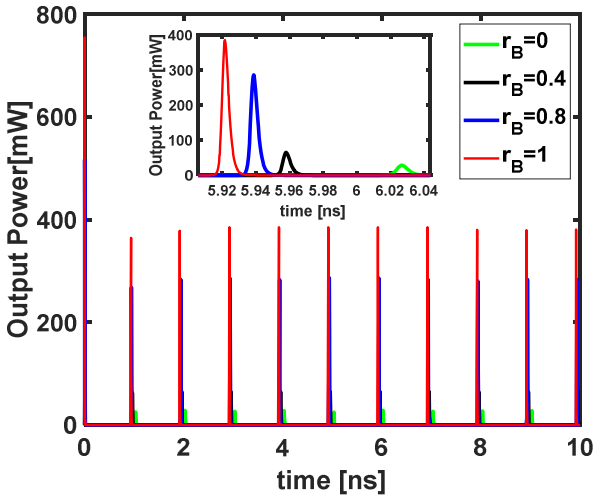


Fig. 6. Comparison of output power in the presence and absence of partial transmission element. With the presence of a partial transmission element, the output power is significantly increased compared to its absence.

## IV. Conclusion

In this article, we investigate and simulate Fano laser dynamics and the effect of PTE on the Fano mirror performance. Also, by placing PTE in the structure of the Fano laser and below the nanocavity, due to the interaction of the waveguide and the nanocavity fields the laser output power is significantly increased. This increase in output power occurs due to the formation of the Fano spectrum in the right mirror reflection spectrum of the laser. The reflection spectrum of the fano mirror indicates that more interaction has been occurred between the waveguide and the nanocavity, and as a result higher reflection level occurs, which enhances the light field inside the laser cavity.

## References


[1] J. Rahimi, V. Ahmadi, and M. H. Yavari, "Modeling and analysis of distributed feedback quantum dot passively mode-locked lasers," *Appl. Opt.*, vol. 55, no. 19, p. 5102, 2016.

[2] S. Arahira, Y. Matsui, and Y. Ogawa, "Mode-locking at very high repetition rates more than terahertz in passively mode-locked distributed-Bragg-reflector laser diodes," *IEEE J. Quantum Electron.*, vol. 32, no. 7, pp. 1211–1224, 1996.

[3] T. S. Rasmussen, Y. Yu, and J. Mørk, "Photonic crystal laser based on Fano interference allows for ultrafast frequency modulation in the THz range," *Nov. In-pl. Semicond. Lasers XVIII*, vol. 10939, 109, p. 9, 2019.

[4] O. Painter *et al.*, "Two-dimensional photonic band-gap defect mode laser," *Science (80-. ).*, vol. 284, no. 5421, pp. 1819–1821, 1999.

[5] T. Baba, D. Sano, K. Nozaki, K. Inoshita, Y. Kuroki, and F. Koyama, "Observation of fast spontaneous emission decay in GaInAsP photonic crystal point defect nanocavity at room temperature," *Appl. Phys. Lett.*, vol. 85, no. 18, pp. 3989–3991, 2004.

[6] H. Altug, D. Englund, and J. Vučković, "Ultrafast photonic crystal nanocavity laser," *Nat. Phys.*, vol. 2, no. 7, pp. 484–488, 2006.

[7] A. R. Zali, M. K. Moravvej-Farshi, and M. H. Yavari, "Small-signal equivalent circuit model of photonic crystal fano laser," *IEEE J. Sel. Top. Quantum Electron.*, vol. 25, no. 6, pp. 1–8, 2019.

[8] S. Matsuo *et al.*, "High-speed ultracompact buried heterostructure photonic-crystal laser with 13 fJ of energy consumed per bit transmitted," *Nat. Photonics*, vol. 4, no. 9, pp. 648–654, 2010.

[9] M. Notomi, K. Yamada, A. Shinya, J. Takahashi, C. Takahashi, and I. Yokohama, "Extremely large group-velocity dispersion of line-defect waveguides in photonic crystal slabs," *Phys. Rev. Lett.*, vol. 87, no. 25, pp. 253902-253902–4, 2001.

[10] T. Baba, "Slow light in photonic crystals," *Nat. Photonics*, vol. 2, no. 8, pp. 465–473, 2008.

[11] W. Xue *et al.*, "Threshold Characteristics of Slow-Light Photonic Crystal Lasers," *Phys. Rev. Lett.*, vol. 116, no. 6, pp. 1–5, 2016.

[12] J. Mork, Y. Chen, and M. Heuck, "Photonic crystal fano laser: Terahertz modulation and ultrashort pulse generation," *Phys. Rev. Lett.*, vol. 113, no. 16, 2014.

[13] U. Fano, "Effects of Configuration Interaction on Intensities and Phase Shifts," *Am. Phys. Soc.*, vol. 124, no. 6, 1961.

[14] M. Heuck, P. T. Kristensen, Y. Elesin, and J. Mørk, "Improved switching using Fano resonances in photonic crystal structures," vol. 38, no. 14, pp. 2466–2468, 2013.

[15] A. E. Miroshnichenko and Y. S. Kivshar, "Fano resonances in nanoscale structures," vol. 82, no. September, pp. 2257–2298, 2010.

[16] C. Kang, S. M. Weiss, Y. A. Vlasov, and S. Assefa, "Optimized light–matter interaction and defect hole placement in photonic crystal cavity sensors," *Opt. Lett.*, vol. 37, no. 14, p. 2850, 2012.

[17] Y. Yu, W. Xue, E. Semenova, K. Yvind, and J. Mork, "Demonstration of a self-pulsing photonic crystal Fano laser," *Nat. Photonics*, vol. 11, no. 2, pp. 81–84, 2017.

[18] T. S. Rasmussen, Y. Yu, and J. Mork, "Theory of Self-pulsing in Photonic Crystal Fano Lasers," *Laser Photonics Rev.*, vol. 11, no. 5, pp. 1–13, 2017.

[19] J. Mork, Y. Yu, T. S. Rasmussen, E. Semenova, and K. Yvind, "Semiconductor Fano Lasers," *IEEE J. Sel. Top. Quantum Electron.*, vol. 25, no. 6, 2019.

[20] B. Tromborg, H. Olesen, X. Pan, and S. Saito, "Transmission line description of optical feedback and injection locking for fabry-perot and dfb lasers," *IEEE J. Quantum Electron.*, vol. 23, no. 11,

pp. 1875–1889, 1987.

[21] Y. Yu *et al.*, “Fano resonance control in a photonic crystal structure and its application to ultrafast switching,” *Appl. Phys. Lett.*, vol. 105, no. 6, pp. 1–15, 2014.

[22] J. Mork *et al.*, “Lasers, switches and non-reciprocal elements based on photonic crystal Fano resonances,” 2017.

[23] A. R. Zali, M. K. Moravvej-Farshi, Y. Yu, and J. Mork, “Small and large signal analysis of photonic crystal fano laser,” *J. Light. Technol.*, vol. 36, no. 23, pp. 5611–5616, 2018.